Phase diagram of a probabilistic cellular automaton with three-site interactions

A. P. F. Atman,* Ronald Dickman,† and J. G. Moreira‡
Departamento de Física, Instituto de Ciências Exactas, Universidade Federal de Minas Gerais, Caixa Postal 702, 30123-970 Belo Horizonte, Minas Gerais, Brazil
(Received 2 October 2002; published 17 January 2003)

We study a (1+1)-dimensional probabilistic cellular automaton that is closely related to the Domany-Kinzel stochastic-cellular automaton (DKCA), but in which the update of a given site depends on the state of *three* sites at the previous time step. Thus, compared with the DKCA, there is an additional parameter p_3 representing the probability for a site to be active at time t, given that it and its nearest neighbors were active at time $t-1$. We study phase transitions and critical behavior for the activity *and* for damage spreading, using one- and two-site mean-field approximations, and simulations, for $p_3=0$ and $p_3=1$. We find evidence for a line of tricritical points in the (p_1,p_2,p_3) parameter space, obtained using a mean-field approximation at pair level. To construct the phase diagram in simulations we employ the growth-exponent method in an interface representation. For $p_3=0$, the phase diagram is similar to the DKCA, but the damage-spreading transition exhibits a reentrant phase. For $p_3=1$, the growth-exponent method reproduces the two absorbing states, first- and second-order phase transitions, bicritical point, and damage-spreading transition recently identified by Bagnoli *et al.* [Phys. Rev. E **63**, 046116 (2001)].

DOI: 10.1103/PhysRevE.67.016107 PACS number(s): 05.10.−a, 02.50.−r, 68.35.Ct, 68.35.Rh

I. INTRODUCTION

Probabilistic cellular automata (PCA) are widely used to model systems with local interactions in physics, chemistry, biology, and social sciences [1–5]. Despite their simplicity, these models exhibit complex behavior and are used to investigate fundamental problems in statistical mechanics, such as spin models [6,7] and nonequilibrium phenomena [8,9]. In particular, the problem of phase transitions in the presence of absorbing states has attracted increasing interest in recent years [10,11]; PCA play a major role in these studies [12–15]. The PCA introduced by Domany and Kinzel [8] is, along with the contact process [16,17], one of the simplest models exhibiting an absorbing-state phase transition

The one-dimensional Domany-Kinzel stochastic cellular automaton (DKCA) is a completely discrete system—temporally, spatially, and in its state space—which attracts interest as a particle system affording a test of ideas on scaling in nonequilibrium critical phenomena [18]. The DKCA has a unique absorbing (''vacuum'') state; its phase diagram presents a critical line separating this absorbing phase from an active one. Continuous phase transitions to an absorbing state are conjectured to belong generically to the directed percolation (DP) universality class [19]. In addition to the active-absorbing transition, Martins *et al.* [20] found a damage-spreading (DS) transition separating the active phase into nonchaotic and chaotic phases. There is numerical evidence that the critical behavior along this transition line also belongs to the DP class, as expected on the basis of universality [21].

Recently, Bagnoli *et al.* [9] introduced a model that can be considered a natural extension of the DKCA: a one-dimensional PCA in which the update of a given site depends on the state of its nearest neighbors and itself, at the preceding time step. (We shall refer to this model as the BPCA.) Thus, compared with the DKCA, there is an additional parameter p_3 representing the probability for a site to be active at time t, given that all three sites were active at time $t-1$. Bagnoli *et al.* studied $p_3=1$, in which case the model presents two absorbing states: the empty one and the completely occupied configuration. As in the DKCA, the density is the order parameter. These authors used the mean-field approximation (at site level), simulations, and field-theoretic arguments to study the model. They found a rich phase diagram, with first- and second-order phase transitions, a bicritical point, and a damage-spreading transition. Except for the line $p_2=1$ in the DKCA, this is the simplest PCA that exhibits a discontinuous phase transition [9].

In this work we extend the analysis of the BPCA considering two cases: the previously studied $p_3=1$, which corresponds to a ferromagneticlike model, and $p_3=0$, representing a *game-of-life*-like model [22,23]. We extend the mean-field analysis to the pair level, and use simulations to construct the phase diagram. In simulations, we apply the growth-exponent method [24] to identify transitions.

This paper is structured as follows. In Sec. II we define the model and its interface representation; the site and pair mean-field approximations are discussed in Sec. III. Simulation results are presented in Sec. IV. We summarize our findings in Sec. V.

II. MODEL

The one-dimensional PCA with three-site neighborhood (BPCA) was proposed by Bagnoli *et al.* [9]. It consists of a ring of L sites $(i=1,2,\ldots,L)$, with periodic boundaries, in which each site i has two possible states, conveniently denoted by $\sigma_i=0,1$. The state of the system at time t is given

*Email address: atman@fisica.ufmg.br
†Email address: dickman@fisica.ufmg.br
‡Email address: jmoreira@fisica.ufmg.br

by the set $\{\sigma_i(t)\}$. In contrast to the deterministic CA studied by Wolfram [1], the present model is a discrete time Markov process: the rules for updating the system are given by transition probabilities. In particular, the state of site i at time $t+1$ depends on $\sigma_{i-1}(t)$, $\sigma_i(t)$, and $\sigma_{i+1}(t)$, via the transition probability $P(\sigma_i(t+1)|\sigma_{i-1}(t),\sigma_i(t),\sigma_{i+1}(t))$. The latter is of totalistic form, i.e., the dependence is through $S_i(t)=\sigma_{i-1}(t)+\sigma_i(t)+\sigma_{i+1}(t)$. Since $S(t)=0$ implies $\sigma_i(t+1)=0$ with probability 1, there remain three free parameters for defining the transition probability. Specifically,

$$P(1|0,0,1)=P(1|0,1,0)=P(1|1,0,0)=p_1,$$

$$P(1|0,1,1)=P(1|1,0,1)=P(1|1,1,0)=p_2,$$

$$P(1|1,1,1)=p_3.$$

Evidently, $P(0|\sigma_{i-1},\sigma,\sigma_{i+1})=1-P(1|\sigma_{i-1},\sigma_i,\sigma_{i+1})$.

Depending on the values of (p_1,p_2,p_3), the asymptotic $(t\to\infty)$ state of the system is either in an absorbing phase (*phase* 0, with all sites in state 0, or *phase* 1, with all sites in state 1), or in the active phase, in which the stationary density ρ of sites in state 1 takes a value different from 0 or 1. Complete determination of the phase diagram in the three-dimensional parameter space is a rather difficult open problem. In this work we focus on two cases: $p_3=1$ and $p_3=0$. In the first case, the model possesses the two absorbing phases cited above, as well as an active phase and a chaotic region (associated with damage spreading). For $p_3=0$, phase 1 is no longer absorbing (though phase 0 of course remains so), and there is again an active phase; the chaotic region is reentrant. $p_3=0$ describes a situation in which "crowding" of individuals leads to their destruction, similar to Conway's game-of-life model [22,23], while $p_3=1$ corresponds to a ferromagneticlike model.

The *absorbing-active* transitions are continuous phase transitions, characterized by critical exponents that belong to the DP universality class. The phase 0–phase 1 transition is discontinuous [9], and the exponents are those of *compact* directed percolation. The DS transitions are also in the DP class, consistent with Grassberger's prediction [21]. The termination of two critical lines at a line of discontinuous transitions marks a *bicritical* point, as has been found in the BPCA for $p_3=1$. For $p_3<1$, phase 1 is no longer absorbing, so that one of the phase boundaries (i.e., between the active and phase 1 absorbing phases) is no longer present. We find (using the two-site mean-field approximation, discussed in Sec. III B) that the bicritical point is actually one terminus of a line of *tricritical* points: for each fixed p_3 in the range $1>p_3>p_3^t\simeq 1/3$, the absorbing-active transition is discontinuous for $(p_1,p_2)<(p_1^t,p_2^t)$ and continuous for larger values, $(p_1,p_2)>(p_1^t,p_2^t)$, where (p_1^t,p_2^t) is the tricritical point. For $p_3\leqslant p_3^t$, the absorbing-active transition is always continuous.

A. Surface representation

The mapping of dynamical systems to a surface-growth representation is an interesting problem, since in many cases the resulting scaling properties are unknown *a priori*. Integration of the local activity (with respect to time) is the most natural procedure. The present method employs the interface representation proposed by de Sales *et al.* [27]. The procedure consists in transforming the spatiotemporal patterns generated by the PCA to a solid-on-solid (SOS) particle deposition. The surface-growth process is attended by kinetic roughening; the associated critical exponents can be measured [13] following the scaling concepts developed by Family and Vicsék [28]. Atman and Moreira [24] demonstrated that the growth exponent β_w exhibits a cusp at criticality, and is very useful for detecting phase transitions.

Height variables are defined by summing the variables $\sigma_i(\tau)$ over the first t time steps:

$$h_i(t)\equiv\sum_{\tau=0}^{t}\sigma_i(\tau). \tag{1}$$

In this way we generate a growth process, with correlations embodied in the roughness $w(L,t)$ [29], defined by

$$w^2(L,t)=\frac{1}{L}\left\langle\sum_{i=1}^{L}[h_i(t)-\overline{h}(t)]^2\right\rangle, \tag{2}$$

where $\overline{h}(t)$ is the mean value of $h_i(t)$ at time t, and $\langle\cdots\rangle$ denotes an average over realizations.

For surface-growth models [29], we expect $w(L,t)$ to follow the scaling form [28]

$$w(L,t)\sim L^{\alpha}f\left(\frac{t}{L^z}\right), \tag{3}$$

where $f(u)$ is a universal scaling function, α is the roughness exponent, $z=\alpha/\beta_w$ the dynamic exponent, and β_w is the growth exponent. The function $f(u)=\text{const}$ for large u, while $f(u)\sim u^{\beta_w}$ for small $u(t\ll L^z)$. At short times, therefore, we expect $w(t)\sim t^{\beta_w}$. It is possible to measure β_w from the slope of a log-log plot of $w(L,t)$ versus t. In the active phase, the roughness does not saturate, growing instead as $w(L,t)\sim t^{1/2}$, corresponding to uncorrelated growth [24], since the correlation length is finite, away from the critical point.

In previous work, Atman and Moreira [24] showed that β_w attains a maximum at the phase transition, and measured its value along the transition line of the DKCA. DP values for others critical exponents in the surface representation of DKCA are verified in Ref. [13].

B. Damage spreading

Martins *et al.* [20] used the DS technique to show that the active phase of the DKCA consists of two phases, chaotic and nonchaotic. The order parameter of this transition is the difference between two replicas initialized with different configurations, but subject to the same sequence of random events during the subsequent evolution. Various prescriptions have been proposed for generating this random sequence for the DKCA [24,25]. In this work, we use the prescription with maximal correlations between the random numbers, as used

TABLE I. BPCA transition probabilities.

$\sigma_i/(\sigma'_{i-1},\sigma'_i,\sigma'_{i+1})$	(1,1,1)	(1,1,0), (1,0,1), or (0,1,1)	(0,0,1), (1,0,0), or (0,1,0)	(0,0,0)
1	p_3	p_2	p_1	0
0	$1-p_3$	$1-p_2$	$1-p_1$	1

in Refs. [20,24]. The issue of how the DS transition line in the DKCA depends on the detailed prescription is addressed in Ref. [26].

In practice, we let the system evolve until it attains a stationary state, and then copy the configuration, introducing some alterations (damage). The two replicas, one with state $\sigma_i(t)$ and the other with state $\varrho_i(t)$, then evolve using the same sequence of random numbers, and the difference between them,

$$\Gamma_i(t)=|\sigma_i(t)-\varrho_i(t)|,$$

is monitored. The fraction of sites in the two replicas with $\sigma_i\neq\varrho_i$ defines their Hamming distance:

$$D_H(t)=\frac{1}{L}\sum_i \Gamma_i(t). \tag{4}$$

The nonchaotic phase is defined as the region of the diagram in which the stationary Hamming distance vanishes for $(L,t)\to\infty$; the chaotic phase is, conversely, the region in which the Hamming distance diverges in the same limit.

To study the chaotic-nonchaotic boundary, we use a slightly different method, in which the *difference* between the replicas is used to generate a *surface-growth process*, as described above. In this case,

$$h_i(t)=\sum_{\tau=0}^{t}\Gamma_i(\tau). \tag{5}$$

Thus, the profile generated by the difference between the replicas behaves just as the profiles at the phase 0–active boundary: the roughness reaches a stationary value in the nonchaotic phase and grows indefinitely in the chaotic phase, with a cusp in the β_w value at the transition.

Since the system has already relaxed to the stationary state when we initiate the damage experiment, creating the damage by randomly altering sites in one copy is likely to perturb the particle density and correlation functions away from their stationary values. This, in turn, would introduce an undesirable asymmetry between the replicas, since the dynamics of damage spreading would be mixed with that of relaxation back to the stationary state (in the copy but not in the original). To avoid such complications, we generate the damage by *rotating* the copy by 180° with respect to the original, with no further modifications, that is, $\varrho(i,t_0)=\sigma(i+L/2,t_0)$, subject to periodic boundary conditions. This represents a large initial damage [a Hamming distance of $\simeq 2\rho(1-\rho)$, with ρ the stationary particle density], which is statistically uniform over the system.

III. MEAN-FIELD THEORY

A. One-site approximation

To begin, we present the mean-field approximation at the site level, for $p_3=1$ and $p_3=0$, and construct the phase diagram from the equations obtained in this approximation. The BPCA is a Markov process in which all sites are updated simultaneously. The configuration $\{\sigma\}$ is a set of stochastic variables with the probability distribution at time t given by $P_t(\sigma)$. The evolution of the latter is governed by

$$P_{t+1}=\sum_{\sigma'}\omega(\sigma|\sigma')P_t(\sigma'), \tag{6}$$

where $\omega(\sigma|\sigma')$ denotes the probability of the transition $\sigma'\to\sigma$, with the properties $\omega(\sigma|\sigma')\geqslant 0$ and $\Sigma_\sigma\omega(\sigma|\sigma')=1$. The transition probability for the BPCA is a product of factors associated with each site:

$$\omega(\sigma|\sigma')=\prod_{i=1}^{L} w_i(\sigma_i|\sigma'), \tag{7}$$

where $w_i(\sigma_i|\sigma')\geqslant 0$ is the conditional probability for site i to be active at time $t+1$, given the configuration σ' at the preceding step. The probabilities w_i are translationally invariant and in fact depend only on the states σ_{i-1}, σ_i, and σ_{i+1} at the previous step:

$$w_i(\sigma_i|\sigma')=w_{3s}(\sigma_i|\sigma'_{i-1},\sigma'_i,\sigma'_{i+1}). \tag{8}$$

We list the w_{3s} in Table I.

Of interest are the n-site marginal probabilities. The evolution of the one-site distribution $P_t(\sigma_i)$ is given by

$$P_{t+1}(\sigma_i)=\sum_{\sigma'_{i-1}}\sum_{\sigma'_i}\sum_{\sigma'_{i+1}} w_{3s}(\sigma_i|\sigma'_{i-1},\sigma'_i,\sigma'_{i+1}) \times P_t(\sigma'_{i-1},\sigma'_i,\sigma'_{i+1}), \tag{9}$$

where $P_t(\sigma'_{i-1},\sigma'_i,\sigma'_{i+1})$ is the marginal distribution for a set of three nearest-neighbor sites. The evolution of the two-site distribution is given by

$$P_{t+1}(\sigma_i,\sigma_{i+1})=\sum_{\sigma'_{i-1}}\sum_{\sigma'_i}\sum_{\sigma'_{i+1}}\sum_{\sigma'_{i+2}} w_{3s}(\sigma_i|\sigma'_{i-1},\sigma'_i,\sigma'_{i+1}) \times w_{3s}(\sigma_{i+1}|\sigma'_i,\sigma'_{i+1},\sigma'_{i+2}) \times P_t(\sigma'_{i-1},\sigma'_i,\sigma'_{i+1},\sigma'_{i+2}). \tag{10}$$

Evidently we have an infinite hierarchy of equations. In the n-site approximation, the hierarchy is truncated by estimating the $(n+1)$-site (and higher) probabilities on the basis of those for n sites.

The simplest case is the one-site approximation, in which $P_t(\sigma'_{i-1},\sigma'_i,\sigma'_{i+1})$ is factored so: $P_t(\sigma'_{i-1},\sigma'_i,\sigma'_{i+1}) = P_t(\sigma'_{i-1})P_t(\sigma'_i)P_t(\sigma'_{i+1})$. This yields the recurrence relation

$$\rho_{t+1}=p_3\rho_t^3+3p_2\rho_t^2(1-\rho_t)+3p_1\rho_t(1-\rho_t)^2, \quad (11)$$

where $\rho_t \equiv P_t(1)$ is the density of active sites (i.e., the order parameter).

Depending on the value of (p_1,p_2,p_3), Eq. (11) admits different stationary solutions, corresponding to the possible BPCA phases discussed above: phase 0 ($\rho=0$), phase 1 ($\rho=1$), and active ($0<\rho<1$). In order to verify the stability of the stationary solutions, we consider a small perturbation in the stationary value ρ^*, $\rho_t=\rho^*+\Delta\rho_t$. Applying this variable change in Eq. (11), we obtain for the mean-field approximation at the site level,

$$\begin{aligned}\Delta\rho_{t+1}=&\Delta\rho_t[3\rho^{*2}(p_3+3p_1-3p_2)+6\rho^*(p_2-2p_1)+3p_1]\\&+(\Delta\rho_t)^2[3\rho^*(p_3+3p_1-3p_2)+3(p_2-2p_1)]\\&+(\Delta\rho_t)^3[p_3+3p_1-3p_2]. \quad (12)\end{aligned}$$

We can write Eq. (12) in a simplified manner,

$$\Delta\rho_{t+1}=a(\rho^*)\Delta\rho_t+b(\rho^*)(\Delta\rho_t)^2+c(\Delta\rho_t)^3,$$

where the coefficients $a(\rho^*)$, $b(\rho^*)$, and c can be associated with the stability of the solutions.

Considering the solution $\rho^*=0$, the stability condition is $a(\rho^*)<1$, which implies $p_1<1/3$. In the case $a(\rho^*)=1$, $(p_1=1/3)$, the solution will be stable only if $b(\rho^*)<0$ and $c<0$; the first condition implies $p_3<2/3$. For $a(\rho^*)=1$ and $b(\rho^*)=0$, the stability of the condition $c<0$ leads to $p_3<1$. Thus, the solution $\rho^*=0$ is always stable for $p_1<1/3$, $p_2<2/3$, and $p_3<1$. The point (1/3,2/3,1) corresponds to a tricritical point in this approximation.

Considering the solution $\rho^*=1$, the stability condition $a(\rho^*)<1$ implies $p_3-p_2<1/3$. In case $a(\rho^*)=1$ ($p_3=p_2+1/3$), the condition $b(\rho^*)<0$ yields $p_2-p_1>1/3$. For $a(\rho^*)=1$ and $b(\rho^*)=0$, the stability condition $c<0$ implies $p_3<1$. So, the point (1/3,2/3,1) is also a tricritical point for the solution $\rho^*=1$! Thus, the point (1/3,2/3,1) corresponds to a *bicritical* point, as Bagnoli *et al.* have already shown. In fact, the solution $\rho^*=1$ is absorbing only for $p_3=1$ (since for $p_3<1$, the dynamics of updating destroys phase 1), and this solution is stable for $p_2>2/3$.

For $0<\rho^*<1$, the stability condition $a(\rho^*)<1$ implies an inequality of second degree in terms of ρ^*. Considering $a=1$, we can solve the corresponding equation, and obtain

$$\rho^*=\frac{(2p_1-p_2)\pm\sqrt{(p_2-2p_1)^2-(p_3+3p_1-3p_2)(3p_1-1)}}{p_3-3p_1-3p_2}.$$

Note that ρ^* vanishes on the line $(1/3,2/3,p_3)$. It is easy to see that the positive solution ρ^*_+ is valid for any (p_1,p_2,p_3), but the negative solution ρ^*_- is valid only for $p_2<2p_1$. Considering the plane $p_1=1/3$, the transition line for $p_2>2/3$ coincides with the vanishing of the square root, since ρ^* must be real. This implies a discontinuous transition for $p_2>2/3$, and the line $(1/3,2/3,p_3)$ corresponds to the tricritical line in (p_1,p_2,p_3) space, in the site approximation.

In the simulations we consider two cases: $p_3=1$ and $p_3=0$. Considering the stability analysis above, we can summarize the phase diagram in these two cases in the following way: for $p_3=1$, Eq. (12) can be written as

$$\rho[(3p_1-3p_2+1)\rho^2+(3p_2-6p_1)\rho+3p_1-1]=0. \quad (13)$$

The three solutions of this equation are the following.

(1) $\rho=0$, phase 0, stable for $p_1<1/3$.

(2) $\rho=1$, phase 1, stable for $p_2>2/3$.

(3) Active phase, for $p_2<2/3$ and $p_1>1/3$, where the stationary density is given by

$$\rho=\frac{3p_1-1}{3p_1-3p_2+1}. \quad (14)$$

For $p_2>2/3$ and $p_1<1/3$, we have a discontinuous transition line separating phase 0 and phase 1 (both stable) at $p_2=1-p_1$.

In case $p_3=0$, we have

$$\rho[(3p_1-3p_2)\rho^2+(3p_2-6p_1)\rho+(3p_1-1)]=0. \quad (15)$$

For this equation there are only two distinct phases.

(1) $\rho=0$, frozen phase, stable for $p_1<1/3$, $p_2\leqslant 2/3$.

(2) Active phase, valid for $p_1>1/3$ and $p_1\neq p_2$, where the stationary density is given by

$$\rho=\frac{6p_1-3p_2\pm\sqrt{9p_2^2-12p_2+12p_1}}{6p_1-6p_2}; \quad (16)$$

the negative root is valid for $p_2<2p_1$, while the positive root is valid for $p_2>2p_1$.

For $p_2>2/3$, the solution of Eq. (16) is either complex or strictly greater than 0, implying a *discontinuous* transition from phase 0 to the active phase, as we anticipate.

The phase diagram in the one-site approximation, for $p_3=1$, is shown in Fig. 1; that for $p_3=0$ is shown in Fig. 2. For $p_3=1$, the phase diagram is as expected [9]. For p_3

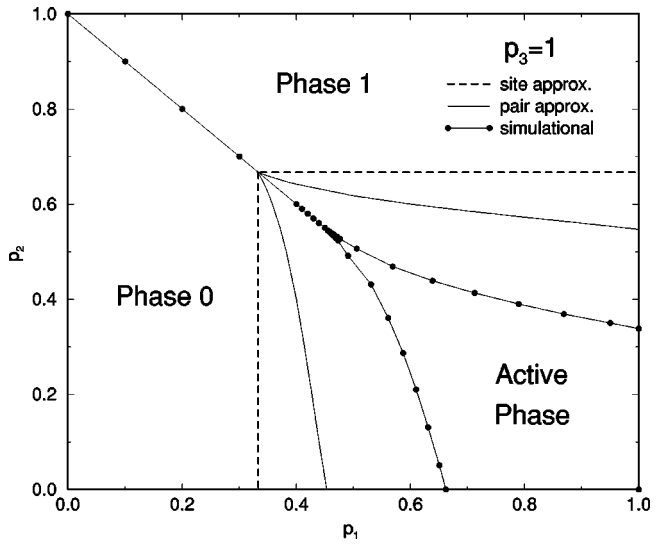

FIG. 1. Phase diagram for the BPCA, $p_3=1$. One- and two-site mean-field approximations are compared with simulation results.

$=0$, we expect a single absorbing state, but the behavior for $p_2>2/3$, where the transition line is discontinuous, is not expected on the basis of simulations. [At the transition the right-hand side of Eq. (16) changes from a complex to a real, nonzero value.]

B. Pair approximation

At the pair level, the probability $P_t(\sigma'_{i-1},\sigma'_i,\sigma'_{i+1},\sigma'_{i+2})$ is factored in the following way:

$$P_t(\sigma'_{i-1},\sigma'_i,\sigma'_{i+1},\sigma'_{i+2}) = \frac{P_t(\sigma'_{i-1},\sigma'_i)P_t(\sigma'_i,\sigma'_{i+1})P_t(\sigma'_{i+1},\sigma'_{i+2})}{P_t(\sigma'_i)P_t(\sigma'_{i+1})}. \tag{17}$$

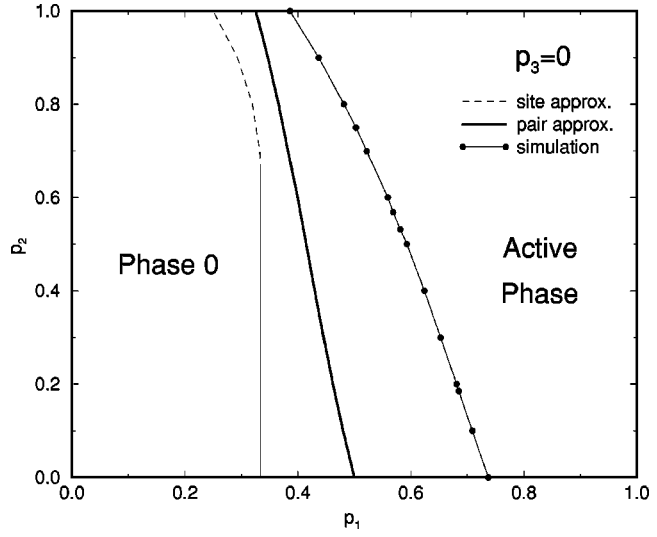

FIG. 2. Phase diagram for the BPCA, $p_3=0$. The mean-field approximation predicts a tricritical point at ($p_2=2/3$, $p_1=1/3$), where a discontinuous boundary (dashed line) meets a continuous transition line.

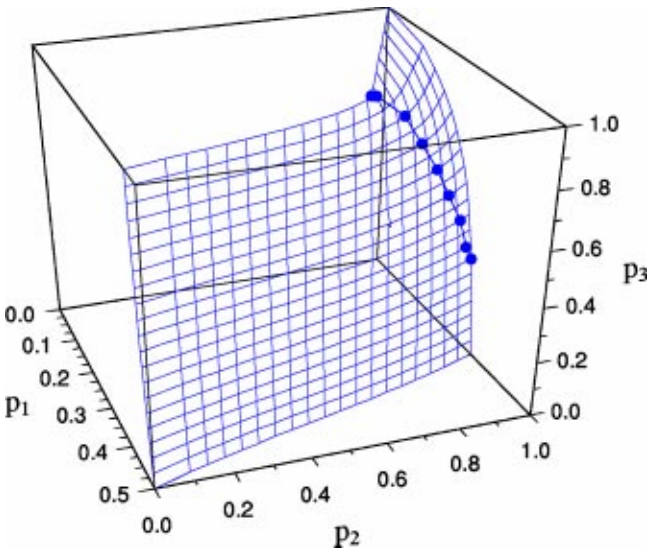

FIG. 3. Line of tricritical points and the critical surface in the (p_1,p_2,p_3) parameter space, as predicted by pair level mean-field approximation. The tricritical line ends near $p_3\simeq 1/3$, while at the site level it extends to $p_3=0$, as shown in Fig. 2.

Calling $z\equiv P(1,1)$, and noting that $P(1)=P(1,0)+P(1,1)$, we can write $P(1,0)=P(0,1)=\rho-z$ and $P(0,0)\equiv 1-2\rho+z$. The recursion relations for the density of active sites ρ and for the density of active pairs z are

$$\rho_{t+1}=p_3\frac{z_t^2}{\rho_t}+p_2(\rho_t-z_t)\left(\frac{2z_t}{\rho_t}+\frac{(\rho_t-z_t)}{1-\rho_t}\right) +p_1(\rho_t-z_t)\left(\frac{2(1-2\rho_t+z_t)}{1-\rho_t}+\frac{(\rho_t-z_t)}{\rho_t}\right), \tag{18}$$

$$\begin{aligned} z_{t+1}=&p_1^2\left(\frac{(\rho_t-z_t)^2(1-2\rho_t+z_t)(2-\rho_t)}{\rho_t(1-\rho_t)^2}\right) \\ &+2p_1p_2\left(\frac{(\rho_t-z_t)}{\rho_t(1-\rho_t)}\right)[z_t(1-2\rho_t+z_t)+(\rho_t-z_t)^2] \\ &+p_2^2\left(\frac{z_t(\rho_t-z_t)^2(1+\rho_t)}{\rho_t^2(1-\rho_t)}\right) \\ &+2p_2p_3\left(\frac{z_t^2(\rho_t-z_t)}{\rho_t^2}\right)+p_3^2\frac{z_t^3}{\rho_t^2}. \end{aligned} \tag{19}$$

Iterating these relations numerically until a steady state is reached, we construct the phase diagram in the pair approximation. Results for $p_3=1$ and $p_3=0$ are shown in Figs. 1 and 2, respectively.

Using the pair approximation, Eqs. (18) and (19), we find numerically the critical surface in the (p_1,p_2,p_3) parameter space and the line of tricritical points, for $p_3<1$, as sketched in Fig. 3. In the region $p_3<1$, phase 1 disappears and the discontinuous absorbing transition lines meet the continuous transition lines at the tricritical points, as shown in Fig. 3. Each one of the eight vertices in this diagram corresponds to

TABLE II. Joint transition probabilities for two BPCA subjected to the same noise.

σ_i,τ_i	(1,1,1;1,1,1)	(1,1,1;1,1,0)	(1,1,1;1,0,0)	
1,1	p_3	$\min(p_2, p_3)$	$\min(p_1,p_3)$	
1,0	0	$b=\max(p_2-p_3,0)$	$b'=\max(p_3-p_1,0)$	
0,1	0	$c=\max(p_3-p_2,0)$	$c'=\max(p_1-p_3,0)$	
0,0	$1-p_3$	$1-\max(p_2,p_3)$	$1-\max(p_1,p_3)$	
σ_i,τ_i	1,1,1;0,0,0	(1,1,0;1,1,0)	(1,1,0;1,0,0)	
1,1	0	p_2	$\min(p_1,p_2)$	
1,0	p_3	0	$b''=\max(p_1-p_2,0)$	
0,1	0	0	$c''=\max(p_2-p_1,0)$	
0,0	$1-p_3$	$1-p_2$	$1-\max(p_1, p_2)$	
σ_i,τ_i	(1,1,0;0,0,0)	(1,0,0;1,0,0)	(1,0,0;0,0,0)	(0,0,0;0,0,0)
1,1	0	p_1	0	0
1,0	p_2	0	p_1	0
0,1	0	0	0	0
0,0	$1-p_2$	$1-p_1$	$1-p_1$	1

a different deterministic rule in the automata studied by Wolfram [1]; for example, ($p_1=1$, $p_2=0$, $p_3=0$) corresponds to the rule 22; ($p_1=1$, $p_2=1$, $p_3=0$) to rule 126; etc.

C. Damage-spreading transition at site level

Bagnoli *et al.* [9] derived a mean-field approximation for the DS transition at $p_3=1$, showing that there is a chaotic region in the active phase of the BPCA. To obtain the one-site approximation for the BPCA at $p_3=0$, we use the approach of Tomé [25]; denoting the configurations by $\{\sigma_i\}$ and $\{\tau_i\}$, the Hamming distance is given by

$$H_t=\langle(\sigma_i-\tau_i)^2\rangle, \tag{20}$$

where the brackets denote an average over realizations. The evolution of the joint probability follows

$$P_{t+1}(\sigma;\tau)=\sum_{\sigma,\tau} W(\sigma;\tau|\sigma';\tau')P_t(\sigma';\tau'), \tag{21}$$

where

$$W(\sigma;\tau|\sigma';\tau') = \prod_i \varpi(\sigma_i;\tau_i|\sigma'_{i-1},\sigma'_i,\sigma'_{i+1};\tau'_{i-1},\tau'_i,\tau'_{i+1}), \tag{22}$$

is the transition probability for the two systems (subject to the same noise), from the state $(\sigma';\tau')$ to $(\sigma;\tau)$. Using the transition probabilities defined in Table I, we can calculate the joint transition probabilities, as shown in Table II.

Now, we can write the equations for the evolution of the order parameter associated with the chaotic transition—the Hamming distance. Denoting the Hamming distance defined by Eq. (4) as $\psi_t\equiv P_t(1;0)=P_t(0;1)$, and using the relation (21), we have

$$\psi_{t+1}=\langle\varpi(1;0|\sigma_{i-1},\sigma_i,\sigma_{i+1};\tau_{i-1},\tau_i,\tau_{i+1})\rangle;$$

using the rules of Table II, we can write ψ_t as

$$\begin{aligned}P_{t+1}(1;0)=&\,p_3P_t(1,1,1;0,0,0)+3p_2P_t(1,1,0;0,0,0)\\&+3(b+c)P_t(1,1,1;1,1,0)\\&+3p_1P_t(1,0,0;0,0,0)\\&+3(b'+c')P_t(1,1,1;1,0,0)\\&+9(b''+c'')P_t(1,1,0;1,0,0).\end{aligned} \tag{23}$$

Setting $P_t(1)\equiv x_t$, we can write $P_t(1;1)=x_t-\psi_t$ and $P_t(0;0)=1-x_t-\psi_t$; thus, using the one-site mean-field approximation $P_t(\sigma_{i-1},\sigma_i,\sigma_{i+1};\tau_{i-1},\tau_i,\tau_{i+1})=P_t(\sigma_{i-1},\sigma_i,\sigma_{i+1})P_t(\tau_{i-1},\tau_i,\tau_{i+1})$, we can write Eq. (23) as

$$\begin{aligned}\psi_{t+1}=\psi_t[&p_3\psi_t^2+3p_2\psi_t(1-x_t-\psi_t)+3p_1(1-x_t-\psi_t)^2\\&+3(b+c)(x_t+\psi_t)^2+3(b'+c')\psi_t(x_t-\psi_t)\\&+9(b''+c'')(x_t-\psi_t)(1-x_t-\psi_t)].\end{aligned} \tag{24}$$

Finally, considering the case $p_3=0$, we have $(b+c)=p_2$, $(b'+c')=p_1$, and $(b''+c'')=|p_1-p_2|$; inserting these values into Eq. (24), we obtain

$$\begin{aligned}\psi_{t+1}=3\psi_t\{&3|p_1-p_2|\psi_t^2+[(p_2-2p_1)-3|p_1-p_2|\\&+3(p_1-p_2)x_t]\psi_t+[(p_1+p_2-3|p_1-p_2|)x_t^2\\&+(3|p_1-p_2|-2p_1)x_t+p_1]\}.\end{aligned} \tag{25}$$

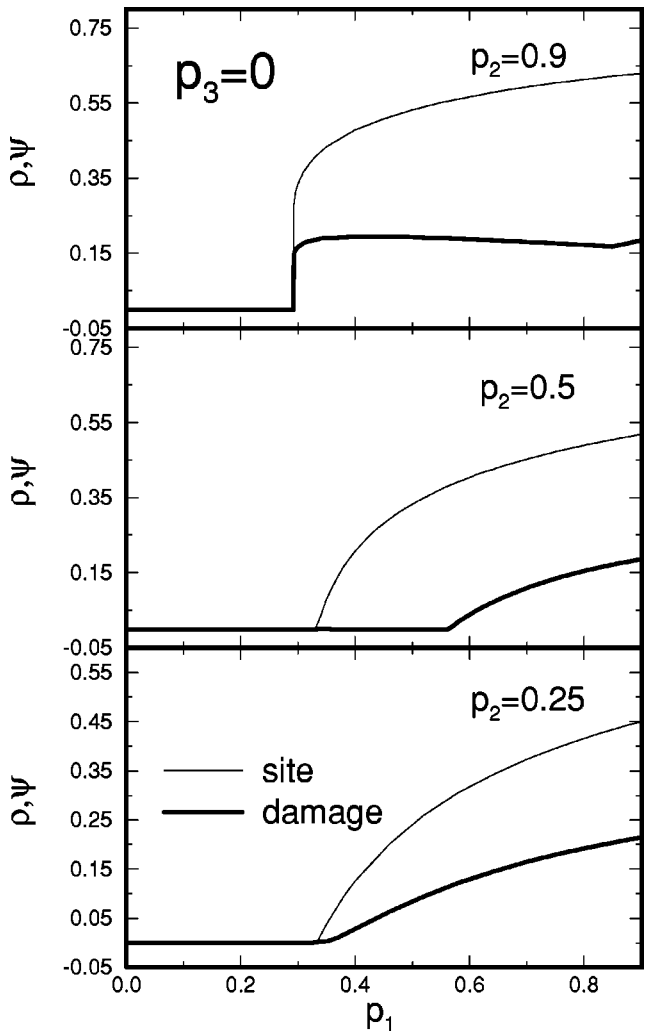

FIG. 4. Density of active sites and Hamming distance, in the mean-field approximation, at site level, for $p_3=0$. Note that for $p_2>2/3$, the transition is discontinuous.

This equation can be iterated numerically using the stationary values of x_t obtained from Eq. (15); there are three possibilities for the joint solutions of Eqs. (15) and (25): $x=\psi=0$, corresponding to phase 0; $x=0$, $\psi\neq 0$, corresponding to the active phase; and $x,\psi\neq 0$, corresponding to the chaotic phase. In Fig. 4 we show the stationary solutions for these equations for some values of p_2. We note that there is a discontinuous DS transition line in this approximation: for $p_2>p_t$ ($p_2=0.9$ in Fig. 4, for example), ψ is always positive if $x>0$. It implies that the DS transition line for $p_2>p_t$ falls on the discontinuous transition analyzed in Sec. III A.

IV. SIMULATION RESULTS

We construct the BPCA phase diagram, for $p_3=0$ and $p_3=1$, using simulations of systems of up to $L=10\,000$ sites (with periodic boundaries), applying the growth-exponent method [24] to locate the transition lines. The initial condition used in the simulations is random, with half the sites occupied. The phase diagrams for absorbing-state transitions are shown in Figs. 1 and 2, for $p_3=1$ and $p_3=0$, respectively. As expected, the pair approximation yields a better prediction than does one-site mean-field theory. Note that for $p_3=0$, the phase diagram is qualitatively the same as for the DKCA [20,24]; the major difference is that the active phase is quite enlarged in the BPCA.

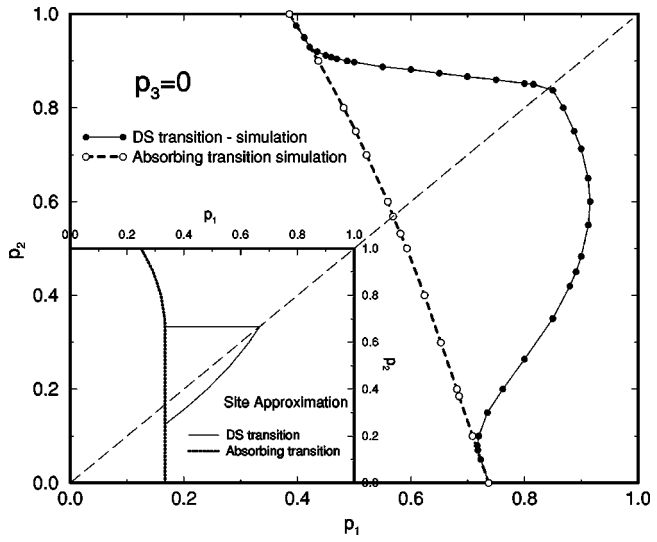

FIG. 5. DS transition line, for $p_3=0$. The one-site mean-field approximation (inset) is compared with simulation data (main graph). Reentrant behavior is observed in both cases.

For $p_3=1$, the pair approximation prediction for the phase boundaries is qualitatively correct, although the bicritical point remains in the same position ($p_1=1/3, p_2=2/3$), as in the site approximation. Simulations place the bicritical point at $(0.460(3),0.540(3))$, but the phase boundaries are in reasonable agreement with the pair approximation prediction. It is important to note that there are only three transitions in this diagram: the phase 0–phase 1 transition (discontinuous) and the phase 0–active and active–phase 1 transitions (continuous). All transitions are located using the growth-exponent method, confirming that this method is able

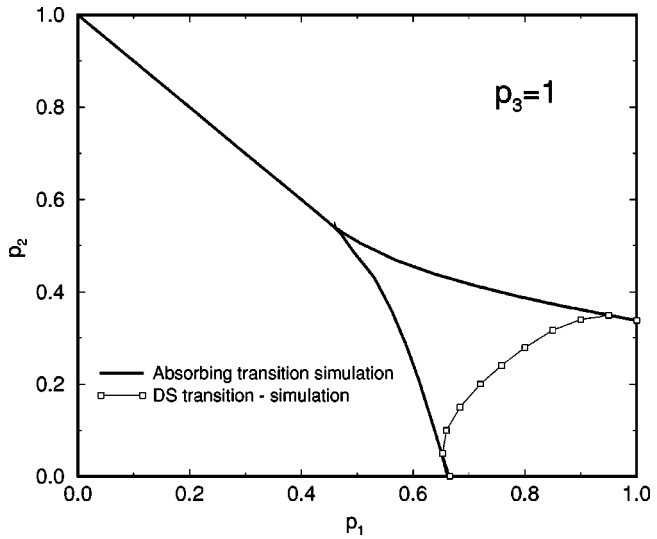

FIG. 6. DS transition line for $p_3=1$. The DS boundary meets the absorbing transition lines for (p_1,p_2) near 1.

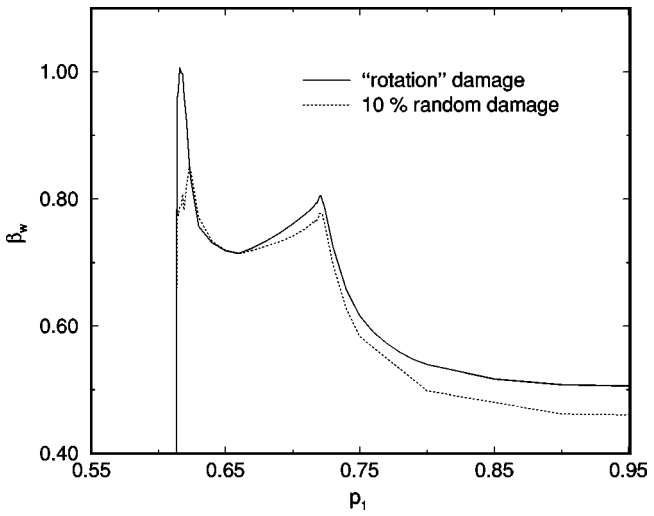

FIG. 7. DS growth exponent for two different initial damages, for $p_3=1$. The left maximum corresponds to the absorbing transition and the right maximum corresponds to the DS transition.

to detect both continuous and discontinuous phase transitions.

The phase diagrams for the DS transition are shown in Figs. 5 and 6, for $p_3=0$ and $p_3=1$, respectively. In the case $p_3=1$, we confirm the results of Bagnoli *et al.*, but some comments are in order. In Ref. [9], the authors sketched several ''damaged domains'' that appear along the active-absorbing phase boundary, and attributed them to the divergence of the relaxation time, or to the fact that small differences in the initial configuration can drive the system to a different absorbing state. As shown in Fig. 7, where we compare the DS transitions obtained using (1) ''rotation'' damage and (2) random damage in 10% of the sites, these domains are only associated with the absorbing-state transition. We see two maxima in the β_w-p_1 curves in Fig. 7: the left maximum, more pronounced, which corresponds to the absorbing-active transition, and the right maximum, which actually corresponds to the nonchaotic-chaotic transition and belongs to the DP class. The left maximum yields an ''apparent'' DS transition, as the ''islands'' of damage commented upon in Ref. [9].

Thus, the left maximum corresponds to the damage domains of Ref. [9], but in fact it is due to the absorbing-active transition: in this region, when the replica is created (in the stationary state), it turns out that only a small region of the ring is active, which results in a constant contribution to the Hamming distance [proportional to $2\rho^*$ with rotation damage, and to $2\rho(t)$ with random damage]. Thus, with rotation damage, the exponent β_w approaches 1 because the system is already in the stationary state, while with the random damage, $\beta_w \sim 0.84$, due to decay of the activity, recovering the DP value. This behavior should not be confused with the *true* damage transition that occurs only at the second maximum, and which corresponds to a unique phase boundary, as shown in Fig. 6.

In the case $p_3=0$, the simulations confirm the reentrant chaotic transition predicted by the one-site mean-field approximation. As shown in Fig. 5, the DS transition line is concave inward toward the active phase, and presents distinct behaviors for $p_1>p_2$ and $p_1<p_2$, as expected. We note that the simulation results suggest a sudden change in the orientation of the active-chaotic phase boundary where the latter crosses the line $p_2=p_1$. Such a discontinuity of slope, clearly evident in the mean-field prediction, may be a consequence of the singular behavior of several transition probabilities on the p_1-p_2 parameter space, as shown in Table II and Eq. (25).

V. CONCLUSIONS

In this work we apply the growth-exponent method in Monte Carlo simulations, and one- and two-site mean-field approximations, to construct the phase diagram of the BPCA for $p_3=1$ and $p_3=0$. The method detects both first- and second-order phase transitions, and also can be used to locate DS transitions. The exponent values indicate that all continuous phase transitions belong to the directed percolation universality class, while the exponent at the discontinuous phase transition agrees with the compact directed percolation value.

We find evidence of a line of tricritical points in the (p_1,p_2,p_3) parameter space, using the mean-field pair approximations. We also find a reentrant chaotic transition for $p_3=0$ in the mean-field approximation, which was confirmed by simulations. These observations illustrate the rich, and at times surprising, phase space structure found in simple nonequilibrium systems.

ACKNOWLEDGMENTS

We thank Franco Bagnoli and Silvio R. Salinas for helpful comments. This work was supported by the Brazilian agencies CNPq and Fapemig.

[1] S. Wolfram, *Theory and Applications of Cellular Automata* (World Scientific, Singapore, 1986).
[2] *Cellular Automata*, edited by D. Farmer, T. Toffoli, and S. Wolfram (North-Holland, Amsterdam, 1984).
[3] *Cellular Automata and Modeling of Complex Physical Systems*, edited by P. Manneville, N. Boccara, G. Vichniac, and R. Bidaux (Springer, Heidelberg, 1989).
[4] *Cellular Automata: Theory and Experiments*, edited by H. Gutowitz (North-Holland, Amsterdam, 1990).
[5] *Cellular Automata and Cooperative Phenomena*, edited by N. Boccara, E. Goles, S. Martinez, and P. Picco, Les Houches Workshop (Kluwer, Academic, Dordrecht, 1993).
[6] F. Bagnoli, J. Stat. Phys. **85**, 151 (1996).
[7] A. Georges and P. Le Doussal, J. Stat. Phys. **54**, 1011 (1989).
[8] E. Domany and W. Kinzel, Phys. Rev. Lett. **53**, 311 (1984).
[9] F. Bagnoli, N. Boccara, and R. Rechtman, Phys. Rev. E **63**,

046116 (2001).
[10] J. Marro and R. Dickman, *Nonequilibrium Phase Transitions in Lattice Models* (Cambridge University Press, Cambridge, 1999).
[11] H. Hinrichsen, Adv. Phys. **49**, 815 (2000).
[12] P. Bhattacharyya, Eur. Phys. J. B **3**, 247 (1998).
[13] A.P.F. Atman, R. Dickman, and J.G. Moreira, Phys. Rev. E **66**, 016113 (2002).
[14] M.J. de Oliveira and J.E. Satulovsky, Phys. Rev. E **55**, 6377 (1997).
[15] S. Kwon, W.M. Hwang, and H. Park, Phys. Rev. E **59**, 4949 (1999).
[16] T.E. Harris, Ann. Prob. **2**, 969 (1974).
[17] R. Dickman and M.A. Muñoz, Phys. Rev. E **62**, 7632 (2000).
[18] W. Kinzel, Z. Phys. B: Condens. Matter **58**, 229 (1985).
[19] P. Grassberger, Z. Phys. B: Condens. Matter **47**, 365 (1982).
[20] M.L. Martins, H.F. Verona de Resende, C. Tsallis, and A.C.N. de Magalhães, Phys. Rev. Lett. **66**, 2045 (1991).
[21] P. Grassberger, J. Stat. Phys. **79**, 13 (1995); H.K. Janssen, Z. Phys. B: Condens. Matter **42**, 151 (1981).
[22] J. Conway, in *What is Life?*, edited by E. Berlejamp, J. Conway, and R. Guy, Winning Ways Vol. 2 (Academic Press, New York, 1982), Chap. 25.
[23] F. Bagnoli, R. Rechtman, and S. Ruffo, Physica A **171**, 249 (1991).
[24] A.P.F. Atman and J.G. Moreira, Eur. Phys. J. B **16**, 501 (2000).
[25] T. Tomé, Physica A **212**, 99 (1994).
[26] H. Hinrichsen, J.S. Weitz, and E. Domany, J. Stat. Phys. **88**, 617 (1997).
[27] J.A. de Sales, M.L. Martins, and J.G. Moreira, Physica A **245**, 461 (1997).
[28] F. Family and T. Vicsék, J. Phys. A **18**, L75 (1985).
[29] A.-L. Barabási and H.E. Stanley, *Fractal Concepts in Surface Growth* (Cambridge University Press, Cambridge, 1995).